

Variability of η Carinae III

Michael Feast¹, Patricia Whitelock² and Freddy Marang²

¹ *Astronomy Department, University of Cape Town, Rondebosch 7701, South Africa.*

email: mwf@artemisia.ast.uct.ac.za

² *South African Astronomical Observatory, PO Box 9, Observatory, 7935, South Africa.*

email: paw@sao.ac.za; fm@sao.ac.za

27 October 2018

ABSTRACT

Spectra (1951-78) of the central object in η Car, taken by A.D. Thackeray, reveal three previously unrecorded epochs of low excitation. Since 1948, at least, these states have occurred regularly in the 2020 day cycle proposed by Damineli et al. They last about 10 percent of each cycle. Early slit spectra (1899-1919) suggest that at that time the object was always in a low state. *JHKL* photometry is reported for the period 1994-2000. This shows that the secular increase in brightness found in 1972-94 has continued and its rate has increased at the shorter wavelengths. Modulation of the infrared brightness in a period near 2020 days continues. There is a dip in the *JHKL* light curves near 1998.0, coincident with a dip in the X-ray light curve. Evidence is given that this dip in the infrared repeats in the 2020 day cycle. As suggested by Whitelock & Laney, the dip is best interpreted as an eclipse phenomenon in an interacting binary system; the object eclipsed being a bright region ('hot spot'), possibly on a circumstellar disc or produced by interacting stellar winds. The eclipse coincides in phase and duration with the state of low excitation. It is presumably caused by a plasma column and/or by one of the stars in the system.

Key words: stars: individual: η Carinae

1 INTRODUCTION

Despite a very extensive literature there is as yet no general consensus on the nature of η Carinae and the cause of the Great Eruption (c. 1838 - 1858) (see Morse et al. 1999 and Davidson & Humphreys 1997 for recent summaries). The present paper is the third in a series reporting observations of this object. The earlier papers are Whitelock et al. 1983 (henceforth Paper I) and Whitelock et al. 1994 (henceforth Paper II). Paper I reported and discussed infrared, *JHKL*, photometry of the object in the years 1972 to 1982 as well as optical and infrared spectroscopy. Paper II continued the photometric series up to 1994 and showed that, besides a gradual increase in brightness over the entire time interval 1972 to 1994, there was evidence for variations on a time scale of about 5 years. This was probably the first convincing evidence for periodicity or quasi-periodicity in the system. Damineli (1996) combined these data with observations of the variations in the He I 10830Å emission line and other spectroscopic results in the literature to suggest that there was a rather stable periodicity of 5.52 years. Later Damineli et al. (1997) found evidence for a variation in the radial velocity of Pa γ emission in this same period. They interpreted this as showing that η Car was a spectroscopic

binary in a highly eccentric orbit and they suggested that various phenomena were associated with periastron passage (see also Damineli et al. 2000). However, Davidson et al. (2000) report HST observations of the central object, which is not resolved from the ground. These do not confirm the velocity behaviour predicted by the Damineli et al. orbit. In the present paper we report an examination of spectroscopic material, particularly that collected by A.D. Thackeray over the years 1951 to 1978, and also give the results of the continued monitoring of η Car in *JHKL*. We discuss these data, as well as published material, with particular reference to the light they throw on the periodicity and nature of the object.

2 PERIODIC SPECTROSCOPIC VARIATIONS

Gaviola (1953) found that there was a marked difference between a spectrum of η Car taken in 1948 and those taken in 1947 and 1949. He I, [Ne III] and various other emission lines of above average excitation were missing in 1948. A similar low excitation event was found to occur in 1965 (Thackeray 1967, Rodgers & Searle 1967). Paper I reported that the object was again in a low excitation state in 1981 at a time

when *JHKL* were near maximum brightness in the ~ 5 year cycle. In the present section we discuss all the spectroscopic studies since 1947 relevant to the high/low excitation state which are known to us, including three previously unreported low states seen on plates taken by A.D. Thackeray.

Thackeray obtained a large number of spectra both of the ‘central object’ (as seen from the ground) and portions of the surrounding (bipolar) ‘homunculus’ and other nebulosity. He published discussions of only a small part of this material though it seems likely that had he lived he would have consolidated his work on this object as he did in the case of RR Tel (Thackeray 1977). There are two main series of his (photographic) spectra. One of these was with the two-prism Cassegrain spectrograph on the Radcliffe (now SAAO) 1.9m reflector. This began on 1951 April 12, soon after the spectrograph was installed and continued, with intermissions, till 1978 February 15, a few days before Thackeray died. The other series, with the coudé grating spectrograph on the same telescope extended from 1960 May 16 to 1974 January 8. All these plates are now in the archives of the SAAO and have been examined. Table 1 lists only those spectra of the central object which are suitable for determining whether it was in a high or low excitation state.

It was found that the spectra could be readily classified using a hand lens and/or a Hartmann spectrocomparator. In this classification one is concerned with the sharp emission lines, not the broad emission lines which underlie many of them. The excitation state was judged using some or all of the following line ratios; 4471He I/4475[Fe II]; 4658[Fe III]/4667[Fe II]; 5876He I/5894Na I; 5754[N II]/5748[Fe II]; 6312[S III]/6318Fe II; and the presence or absence of 3869,3967[Ne III]. The strength of the Balmer absorption lines was also taken into account. Damineli’s (1996) work indicates that the equivalent width of 10830He I varies continuously through the 5.52 year cycle as does the *JHKL* brightness. It may be somewhat surprising therefore that it was possible on the basis of the above criteria to classify the sharp-line spectra unambiguously as belonging to either the normal (high excitation) state or the low state. However, the 10830He I does not necessarily arise entirely in the same region as the sharp line spectra. Furthermore, as the referee has pointed out to us, the time interval over which 10830A practically disappears is relatively short and well defined. There is only one spectrum (Cb1567) in which the ratio 4471He I/4475[Fe II] suggests a possible intermediate state and even this is somewhat uncertain. This is not to say that all the spectra assigned to a particular state are identical. Differences between such spectra are suspected and indeed were already noted between the high states of 1947 and 1949 by Gaviola (1953). However, any such differences are minor compared with the high/low state differences.

Table 2 lists other post-1947 results on high/low states from the literature. In Tables 1 and 2 the date is given, as well as the cycle and phase of each spectrum (ϕ), based on the relation;

$$\phi = (JD - 2430661)/2020. \quad (1)$$

Where JD is the Julian date. This uses the period and date of supposed periastron passage (\approx time of conjunction) in the orbit of Damineli et al. (2000). We test this period below. In view of the work of Davidson et al. (2000) which

Table 1. Spectral State (Thackeray)

Plate	Date	Phase	State
Ca9	12.4.51	1.529	H
Cc40	29.4.51	1.537	H
Cc63	8.5.51	1.542	H
Cb99	29.5.51	1.552	H
Cb100	29.5.51	1.552	H
Ca109	2.6.51	1.554	H
Cc135	11.6.51	1.559	H
Ca142	14.6.51	1.560	H
Cb204	7.7.51	1.572	H
Cb208	10.7.51	1.573	H
Ca896	26.6.52	1.747	H
Cb1567	28.6.53	1.929	I?
Cb1821	30.12.53	2.021	L
Cb1960	12.5.54	2.086	L
Cc2313	24.2.55	2.229	H
Ca2385	6.4.55	2.249	H
Ca2430	11.5.55	2.267	H
Cb2889	15.5.56	2.450	H
Cb3246	14.5.59	2.991	L
Cb4291	1.6.59	3.000	L
Cc4661	6.2.60	3.124	H
Cb4714	23.3.60	3.147	H
Cb5086	21.5.61	3.357	H
Cb5263	3.1.62	3.469	H
Cb5787	2.5.63	3.709	H
Cb6193	2.3.64	3.860	H
Cc6713	24.3.65	4.051	L
Cc7171	2.3.66	4.221	H?
Cc7210	22.3.66	4.231	H
Cb8205	4.6.68	4.629	H
Cc8843a	25.5.70	4.986	L
Cb8846b	4.6.70	4.991	L
Cb9251	15.2.78	6.383	H
DZ10	16.5.60	3.174	H
DZ31	18.5.60	3.175	H
DZ43	8.6.60	3.185	H
DZ52	9.6.60	3.185	H
DY81	8.7.60	3.200	H
DZ177	31.1.61	3.302	H
DZ178	31.1.61	3.302	H
DY646	18.5.62	3.536	H
DZ658	20.5.62	3.537	H
DZ1310	19.3.65	4.049	L
DZ3041	2.1.72	5.276	H
DZ3601	14.6.73	5.538	H
DY3726	8.1.74	5.641	H

Notes to Table 1:

Ca; 20 A/mm at H γ

Cb; 29 A/mm at H γ

Cc; 49 A/mm at H γ

Coudé (D) Series

DY; 13.6 A/mm (1st order); 6.7 A/mm (2nd order)

DZ; 31 A/mm (1st order); 15.6 A/mm (2nd order)

was mentioned in the Introduction, one is not constrained in adopting any specific interpretation of the adopted zero-phase. At least initially, it can be considered as simply a convenient reference point. In a few cases Table 2 shows that only the year and month of the observation were published. The phase given then corresponds to the middle of the month. The phase is thus uncertain in these cases by ~ 0.007 . In no case is this of significance in the discussion.

Table 2. Spectral State (Misc)

Date	Phase	State	ref
27.6.47	0.843	H	1,2
19.4.48	0.990	L	1,2
16.7.49	1.215	H	1,2
30.4.61	3.346	H	3
1.5.61	3.347	H	3
2.5.61	3.347	H	3
-3.64	3.866	H	4
-2.65	4.032	L	4
-2.66	4.211	H	4
10.3.74	5.672	H	5
21.5.81	6.973	L	6
-6.81	6.986	L	7
31.10.81	7.054	L	8
1.11.81	7.054	L	8
2.11.81	7.055	L	8
24.12.81	7.080	L	5
-.12.82	7.256	H	7
21.2.83	7.290	H	5
4.4.85	7.673	H	6
22.3.86	7.847	H	9
-1.87	7.996	L	7
15.1.87	8.024	L	10
20.6.92	8.977	L	11
18.11.97	9.956	H	12
24.11.97	9.958	H	13
18.12.97	9.970	L	13
25.12.97	9.974	L	12
6.3.98	10.008	L	13
23.3.98	10.018	L	12
3.7.98	10.067	H	13

References:

- 1 Gaviola (1953)
- 2 Viotti (1968)
- 3 Aller & Dunham (1966)
- 4 Rodgers & Searle (1967)
- 5 Zanella, Wolf & Stahl (1984)
- 6 Bidelman, Galen & Wallerstein (1993)
- 7 Damineli et al. (1994)
- 8 Paper I
- 9 Hillier & Allen (1992)
- 10 Altamore, Maillard & Viotti (1994)
- 11 Damineli et al. (1998)
- 12 McGregor, Rathborne & Humphreys (1999)
- 13 Wolf et al. (1999)

The data from Tables 1 and 2 are shown plotted in Figs. 1 and 2. Fig. 1 shows all the data whilst Fig. 2 shows the data for phases 0.8 to 0.2 on a larger scale. The numbers are modified cycle numbers to avoid changing the cycle at phase zero, in the middle of the low state. Thus, for example, spectra with phases between 3.5 and 4.5 in the tables are plotted as cycle number 4. The plot is clearly consistent with the recurrence of the low excitation state in a periodicity close to that proposed by Damineli et al. (2000) (which is, of course, partly based on some of these data). In particular the three previously unreported low states in Thackeray's data (1953-4, 1959, 1970) which are plotted as cycles 2, 3 and 5, fall in the same phase range as the previously known low states. No low states have been found between phases 0.1 and 0.9.

Detailed examination of Fig. 2 shows that the phenomena do not repeat exactly. There is a high state (cycle 10) at

phase .067 whilst there are low states at phase .080 (cycle 7) and .086 (cycle 2). If one adjusted the period to remove this apparent anomaly then the high excitation point in cycle 10 at phase .958 would be moved to a phase greater than the low excitation point in cycle 7 currently shown at phase .977. Some caution is necessary in this discussion since the criteria used (or their application) may not have been exactly the same for all the spectra, especially for the results of different authors which are taken from the literature. Note that the intermediate point in Fig. 2 at phase .929 (cycle 2) is the only spectrum in Table 1 which suggests an intermediate classification. This depends on a $\lambda 4471\text{He I}/4475[\text{Fe II}]$ estimate of low weight. $\lambda 4471$ is present (in a low state it is absent on these spectra) and it is quite possible that the spectrum should actually be classified as in the high state. Leaving aside this intermediate point, the low state points in cycle 7 show that some, and perhaps all, low states extend over a phase range of at least 0.1. However, the high excitation phase points in cycle 10, if typical, show that the low state phase range cannot be significantly greater than this. Bearing in mind some possible variation from cycle to cycle, we may conclude from Fig. 2 that the low state extends from phase ~ 0.970 to phase ~ 0.085 and is centred at phase ~ 0.025 which is about 50 days after periastron in the Damineli et al. (2000) supposed orbit. The results of this section are further discussed in section 6.

3 EARLY SLIT SPECTRA

Walborn & Liller (1977) have discussed early (19th century) objective prism spectra of η Car. Particularly important is the 1893 spectrum which shows an F-type absorption spectrum. The first known slit spectrum was obtained with the McClean (Victoria) telescope at the Cape in 1899 and was described by Gill (1901). This is listed in Table 3 together with two plates (also with the McClean telescope) of 1919 discussed by Lunt (1919), plates of 1912-1914 from the Lick Southern station (Moore & Sanford 1913) and three Cape (McClean) plates of 1923. The 1899 plate could not be located but is reproduced in Gill's paper. The two 1919 plates are in the SAAO archives and were examined (one is reproduced in Lunt's paper). The 1923 plates are recorded in the McClean plate book but are missing from the archives. They do not seem to have been described in print. The SAAO archives also have glass copies of the 1912-14 Lick plates including one well exposed plate not discussed by the Lick workers. These glass copies were apparently sent by G. Herbig to A.D. Thackeray.

The Cape 1919 plates and three of the Lick plates are of good quality, as can be seen in the reproductions of some of them in the references cited above. The spectra are striking in that although they are generally similar to the more recent ones described in section 2, they all have 4471He I missing and can clearly be classified as in a low excitation state. In the 1919 plates it is possible that $4658[\text{Fe III}]$ is weakly present, but this is not certain. Gill's (1901) line list of the 1899 plate at first looks surprising since he measured a line at 4471.3 \AA . However, this spectrum (a 6 hour 10 min exposure over parts of 4 nights) was obtained during the test phase of a new spectrograph and suffered from thermal instability problems. $[\text{Fe II}]$ and Fe II lines in the region of 4471 show

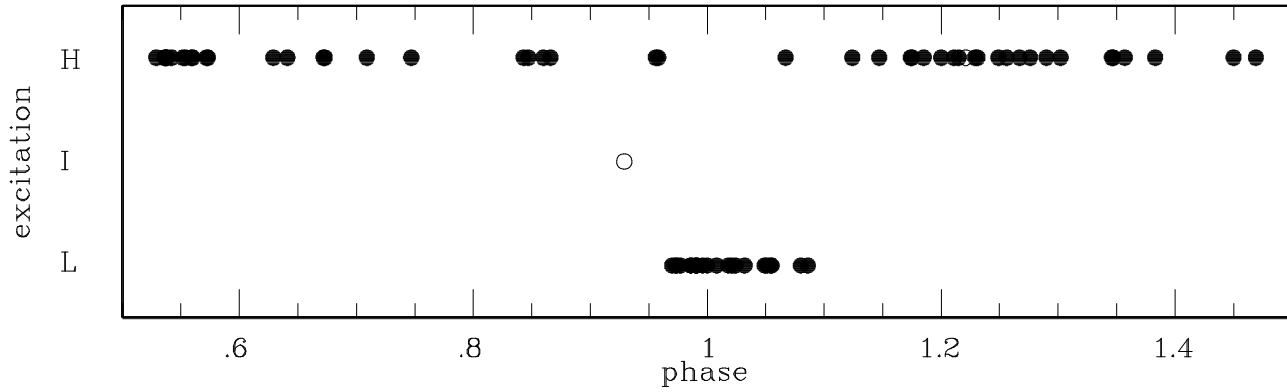


Figure 1. The data from Tables 1 and 2 showing the high (H), Intermediate (I) and low (L) states of ionization plotted against phase in the 2020 day cycle. The open circles represent the two less certain assignments.

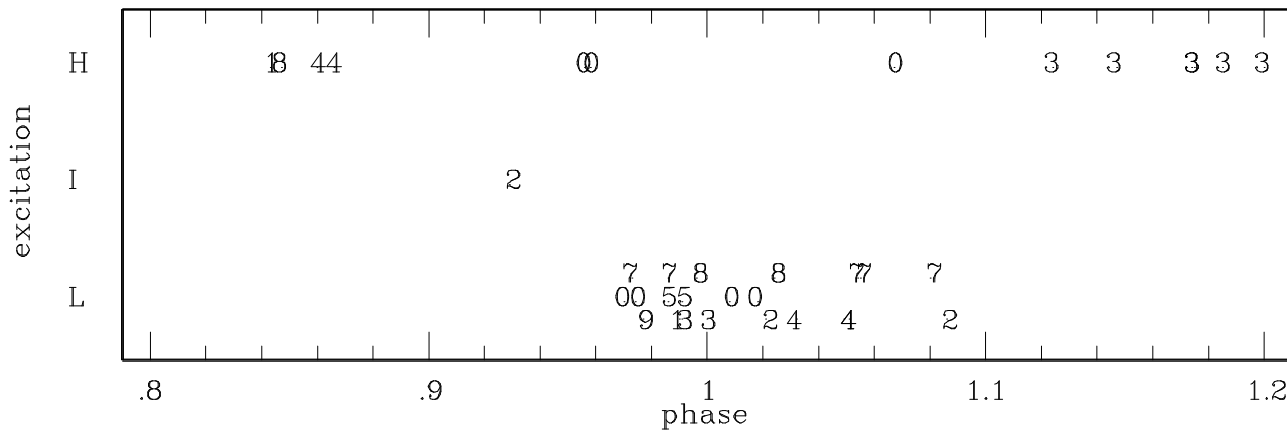


Figure 2. As for Fig. 1, but for the restricted phase range, 0.8 to 0.2. The cycle numbers defined in the text are shown (cycle 10 shown as 0). The L state positions are spread vertically for clarity.

that Gill’s wavelengths are $\sim 2\text{\AA}$ too small so that the true wavelength of the line is ~ 4473.3 . Aller & Dunham (1966) measured emission lines in a 1961 spectrum at 4472.9 Fe II (Intensity 4) and 4474.9 [Fe II] (Intensity 9). It is likely that Gill’s ‘4471’ is a blend of these lines, especially as the ratio $\text{Fe II}/[\text{Fe II}]$ was probably greater in Gill’s time than in 1961 (see section 4).

Table 3 shows the phases of the early plates using the Daminieli et al. (2000) elements (equation 1). It is clear that these are incompatible with the restricted phase range of low excitation states shown in Fig. 2. It would require a large period change (to ~ 2150 days) to change the phase of the 1913-19 observations to near zero and this would be inconsistent with the discussion in sections 2 and 5 and with the 1899 spectrum.

We can conclude that whilst the low excitation states have occurred regularly every ~ 2020 days for the last 50 years at least, the situation was quite different 30 years before that. It seems reasonable to assume that at these earlier times the spectrum of the central object as viewed from the ground was always in the low state. This result, together with the secular trends noted in the next section must obviously be taken into account in any complete model of the system.

Note that Gill (1901) also describes an objective prism

Table 3. Early Slit Spectra

Date	Phase	4471	Ref
14-17.4.1899	0.129	(no)	1
29.3.1912	0.471	-	2
11.3.1913	0.642	no	2
28.3.1913	0.651	no	2
2.3.1914	0.818	-	2
2.3.1914	0.818	-	2
11.3.1914	0.823	no	3
20-23.2.1919	0.718	no	4
14-17.4.1919	0.745	no	4
15.6.1923	0.498	-	5
18.6.1923	0.499	-	5
19.6.1923	0.500	-	5

References:

- 1 Gill 1901
- 2 Moore & Sanford 1914
- 3 Lick (unpublished)
- 4 Lunt 1919
- 5 Cape (missing plates)

plate of 1899 January, and Spencer Jones (1931) one of 1919 April. The SAAO archives contain objective prism plates taken in May 1901. If slit spectra taken in the period 1919-

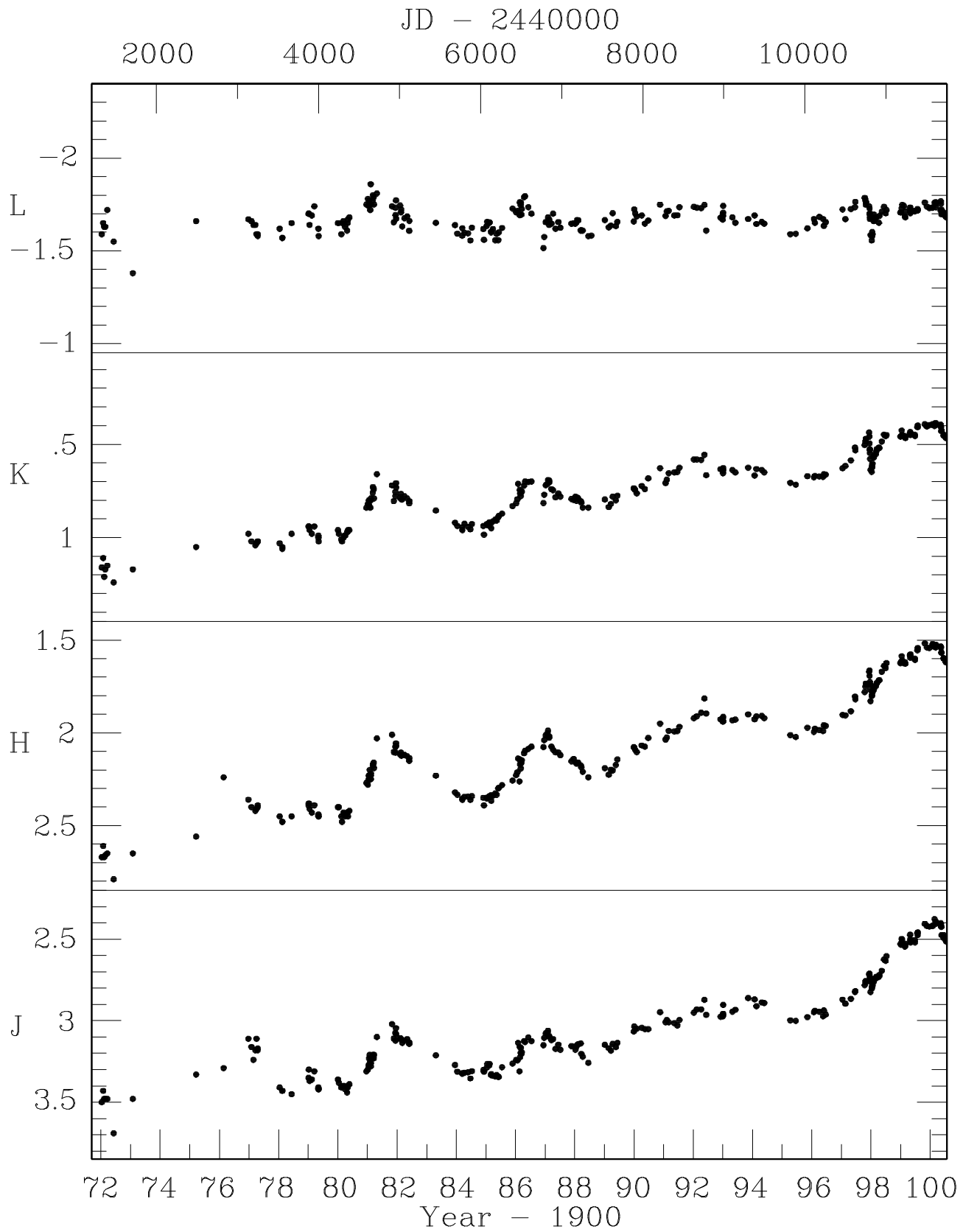


Figure 3. Infrared light curves in *JHKL* for 1972-2000.

1947 exist they would be very valuable. We are not, however, aware of any.

4 LONG TERM SPECTRAL CHANGES

Baxandall (1919) and Lunt (1919) noted differences between the Cape spectrum of 1899 and those of 1912-14 (Lick) and 1919 (Cape). Using modern identifications these indicate that the Fe II/[Fe II] and Ti II/Fe II emission line ratios were greater in 1899 than later. Thackeray (1953) noted that Ti II emission was weaker in 1951-53 than in 1919. he also noted (Thackeray 1967) that in 1961-5 Ti II absorption was stronger than in Gaviola's 1949 observations.

It was shown in Paper I that 2.06 μ m He I emission was stronger in 1983, at phases 0.924, 0.950, and 0.082, than in the 1968 observation of Westphal & Neugebauer (1969) at phase 0.646. Since Daminieli (1996) shows that the equivalent width of 10830 He I emission is a minimum near phase zero, one would have expected the opposite unless the strength of He I were increasing with time. This together with the results of the last section suggest a secular increase in the strengths of high excitation lines (He I etc.). Other evidence for this is briefly summarized by Daminieli et al. (1999).

In contrast, Paper I also showed that the equivalent width of Br γ was about the same in 1981 as 1968. Daminieli et al. (1997) found that Pa γ varied little in strength with respect to the continuum in the 2020 day cycle. These results suggest that the hydrogen emission varies with the continuum both in the cyclical variations and with a secular trend. Note, however, that Aitken et al. (1977) who observed at phase 0.08 in 1976 found Br γ to be only half the strength of that found in Paper I at about the same phase in 1981. This might be due to the fact that Aitken et al. used a much smaller aperture (3.4×4.8 arcsec) than either Westphal & Neugebauer or Paper I; although in Paper I no difference was found between observations though apertures of 12 and 36 arcsec.

5 INFRARED PHOTOMETRY

Monitoring of η Car in *JHKL* at SAAO in the period 1972-94 established a quasi-cyclical variation with a period of the order of 5 years superposed on a secular increase in brightness (see Paper II). Table 4 contains the results of a continuation of this series of observations for the period 1994-2000. As in all recent work in this series, the observations were made with the SAAO MkII photometer on the 0.75m reflector at SAAO, Sutherland and using a 36 arcsec diaphragm. The individual results are accurate to better than ± 0.03 in *JHK* and ± 0.05 in *L*. The results are in the system defined by the standard stars of Carter (1990).

Fig. 3 shows the photometry for the period 1972-2000. The secular increase in brightness has continued and its rate has increased (see Davidson et al. 1999). This long term brightening is most marked at *J*. The maximum in the 2020 day cycle expected near 1998.0 is not seen in *JHK*. In fact, the light curves peak only in early 2000 where this data set ends. This can be plausibly attributed to the increased rate of secular brightening. Perhaps the most striking feature of

Table 4. Near-Infrared Photometry

JD-2440000 (day)	<i>J</i>	<i>H</i>	<i>K</i>	<i>L</i>
	(mag)			
9379.52	2.869	1.927	0.667	-1.691
9402.54	2.910	1.911	0.632	-1.645
9468.41	2.887	1.909	0.638	-1.656
9498.30	2.890	1.920	0.650	-1.647
9820.32	2.997	2.012	0.706	-1.590
9887.31	3.001	2.023	0.716	-1.592
10031.58	2.977	1.972	0.671	-1.621
10111.58	2.948	1.995	0.677	-1.672
10123.53	2.938	1.977	0.669	-1.651
10178.39	2.944	1.984	0.672	-1.684
10224.42	2.973	1.991	0.675	-1.672
10234.22	2.937	1.959	0.660	-1.635
10256.26	2.962	1.962	0.662	-1.655
10464.57	2.870	1.903	0.629	-1.723
10499.49	2.895	1.905	0.616	-1.671
10567.36	2.865	1.883	0.586	-1.725
10618.19	2.823	1.804	0.518	-1.736
10623.30	2.817	1.819	0.533	-1.764
10738.62	2.781	1.780	0.504	-1.786
10746.62	2.758	1.750	0.484	-1.774
10750.62	2.756	1.734	0.472	-1.749
10755.62	2.760	1.741	0.470	-1.761
10792.56	2.714	1.671	0.437	-1.740
10796.50	2.710	1.663	0.458	-1.699
10798.44	2.719	1.693	0.495	-1.728
10800.49		1.738	0.528	
10801.53	2.731	1.725	0.528	-1.702
10802.61	2.742	1.735	0.547	-1.672
10805.61	2.758	1.766	0.578	-1.682
10809.60	2.824	1.829	0.638	-1.585
10824.57	2.802	1.801	0.648	-1.556
10827.56	2.794	1.798	0.620	
10830.56	2.765	1.780	0.613	-1.602
10831.52	2.789	1.783	0.622	-1.580
10833.59	2.782	1.780	0.603	-1.590
10848.55	2.749	1.760	0.567	-1.697
10849.63	2.762	1.768	0.572	-1.660
10850.65	2.753	1.754	0.566	-1.665
10852.56	2.753	1.762	0.563	-1.666
10877.61	2.738	1.747	0.552	-1.678
10879.48	2.730	1.738	0.538	-1.681
10887.47	2.734	1.731	0.526	
10912.38	2.730	1.718	0.518	-1.651
10918.36	2.720	1.716	0.520	-1.688
10948.30	2.693	1.670	0.485	-1.710
10976.22	2.624	1.639	0.448	-1.737
10996.20	2.633	1.650	0.457	-1.702
11006.28	2.603	1.623	0.450	-1.720
11179.61	2.528	1.623	0.458	-1.707
11186.56	2.534	1.616	0.456	-1.709
11194.62	2.498	1.586	0.426	-1.729
11200.62	2.503	1.609	0.452	-1.748
11221.63	2.535	1.623	0.458	-1.742
11233.48	2.545	1.618	0.457	-1.687
11238.41	2.528	1.625	0.461	-1.714
11239.48	2.540	1.627	0.467	-1.680
11298.25	2.472	1.581	0.441	-1.734
11299.49	2.500	1.583	0.434	-1.711
11300.30	2.510	1.595	0.450	-1.704
11302.26	2.520	1.576	0.449	-1.723
continued ...				

Table 4. continued

JD-2440000 (day)	<i>J</i>	<i>H</i>	<i>K</i>	<i>L</i>
	(mag)			
11355.28	2.504	1.599	0.449	-1.714
11358.21	2.519	1.607	0.456	-1.715
11389.19	2.461	1.555	0.408	-1.725
11391.19	2.473	1.544	0.408	-1.718
11392.19	2.457	1.543	0.399	-1.721
11479.60	2.405	1.517	0.393	-1.761
11501.60			0.403	
11505.61	2.419	1.540	0.405	-1.739
11536.60	2.422	1.542	0.397	-1.730
11572.57	2.418	1.530	0.396	-1.732
11575.55	2.419	1.521	0.393	-1.734
11599.47	2.376	1.536	0.402	-1.760
11613.37	2.392	1.539	0.386	-1.762
11615.34	2.392	1.525	0.394	-1.754
11617.41	2.403	1.527	0.396	-1.735
11674.27	2.411	1.535	0.394	-1.718
11676.27	2.401	1.535	0.407	-1.768
11678.29	2.413	1.541	0.405	-1.754
11683.34	2.424	1.567	0.430	-1.723
11685.39	2.474	1.567	0.424	-1.697

the light curves is the marked dip near 1998.0 which was originally noted by Whitelock & Laney (1999). This is illustrated in more detail in Fig. 4. The minimum of this dip occurs between JD 2450809 and 2450824 and is evidently within a few days of JD 2450815. This is at phase 0.977 or 46 days before zero-phase on the Daminieli et al. elements (equation 1). Fig. 5 compares the region near zero-phase in this cycle (cycle 10) at *K* with the observations in the two previous cycles. Unfortunately the observations are sparse at these earlier epochs. Nevertheless, there is a drop in brightness consistent with the beginnings of a dip in the cycle 9 data and of an emergence from a dip in the cycle 8 data. In cycle 7 there is a gap of more than 180 days in the data at the crucial phase and before that the data are too sparse to use in identifying dips. The predicted minimum in cycle 8 is at JD 2446775 which is in fact the date of the faintest point in this cycle. Thus if the dip occurs with strict regularity the period cannot be less than 2020 days. The predicted minimum in cycle 9 is at JD 2448795, whilst the faintest point is at JD 2448783. Thus the period cannot be made longer by more than 12 days at the most. It may therefore be concluded that although the data are rather sparse except in cycle 10, the evidence from cycles 8 and 9 indicates that the dip does occur regularly with a period close to 2020 day. Note that although the above discussion refers to the *K* magnitudes the results are the same in the other three colours.

Since the *L* magnitude is less affected by the secular trend than *JHK*, one can more safely look at the 2020 day variations at this wavelength. Fig. 6 shows the *L* data folded on this period with a linear trend removed and with a third order sine curve fitted. The scatter ($\sigma = 0.042$ mag.) apparent in this plot is partly real and partly observational. The fitted curve is relatively flat except for a ‘hump’ between phases ~ 0.7 and 0.2 , which also contains the dip.

The dip shown by the infrared observations (Fig. 4) is at about the same phase as that shown by the X-ray observations (Ishibashi et al. 1999). The principal difference

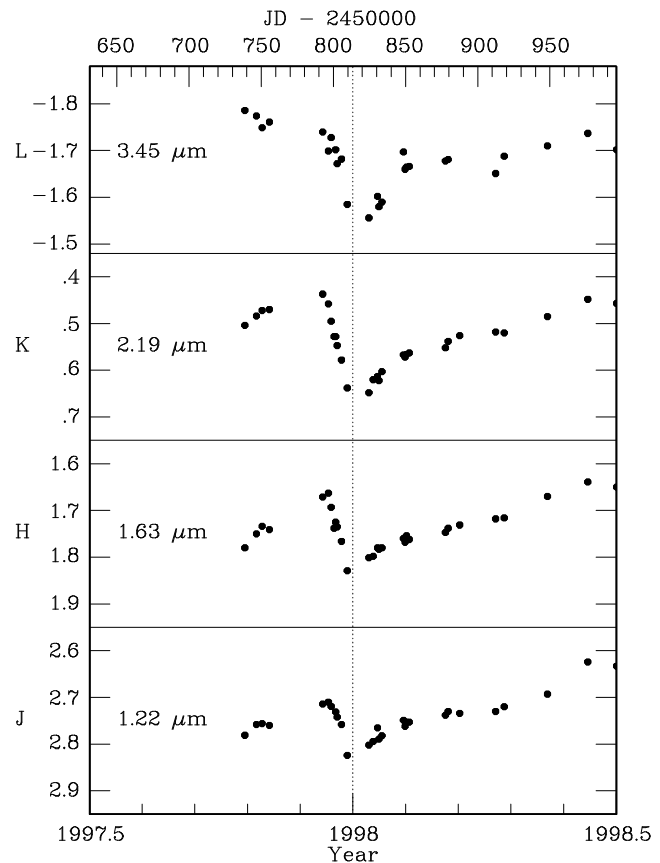


Figure 4. Infrared light curves in *JKHL* near the time of the 1998 dip. The minimum in the dip (phase 0.977) is shown by the vertical line.

being that the X-ray dip is much deeper. The dip in *J* begins about 35 days (0.017 of a cycle) later than that in the X-rays and coincides with the phase at which the X-rays reach minimum. Note that the epoch of minimum increases slightly with increasing wavelength through the infrared as can be seen from Fig. 4. This together with the X-ray results suggests a possible general dependence of the phase of the dip on wavelength. However, the effect in the infrared may be due, at least partially, to the steeper secular increase in brightness at the shorter wavelengths. There is also a small dip in the visual light curve (van Genderen et al. 1999), though the relevant epoch is not well enough sampled to define its depth and shape.

Fig. 7 shows the *L* light curve for phases 0.8 to 0.2 with the linear trend and the third order sine curve shown in Fig. 6 removed. The dip is seen to extend from phase ~ 0.96 to ~ 0.06 . The centre of the dip is at phase ~ 0.01 and the deepest point at phase 0.977 (the point shown at this phase in Fig. 7 is from cycle 8 at JD 2446775). The asymmetric shape of the dip (steep drop, slower rise) is qualitatively similar to that shown by the X-rays (Ishibashi et al. 1999).

6 DISCUSSION

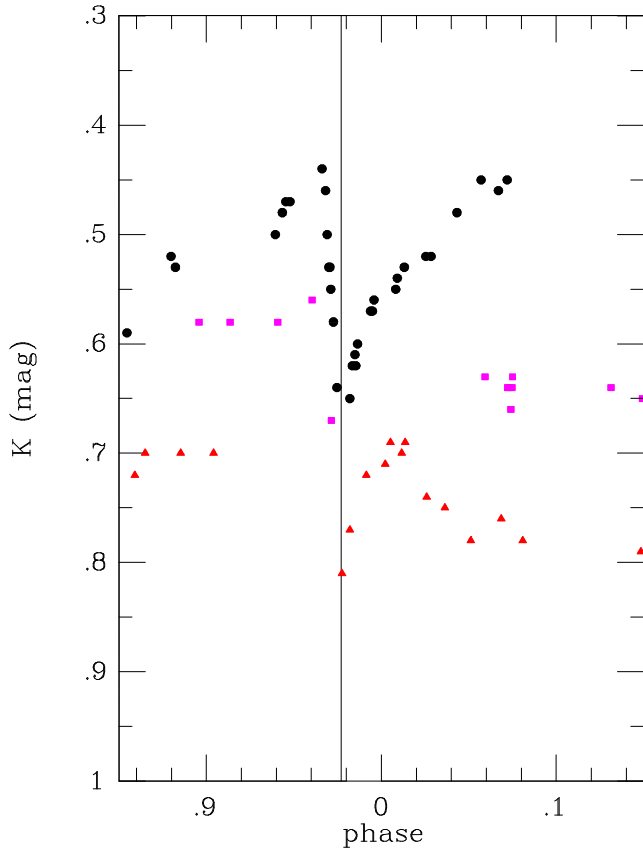


Figure 5. The light curve at K near phase 0.0 at several epochs, triangles - cycle 8; squares - cycle 9; filled circles - cycle 10. The vertical line shows the time of minimum (phase 0.977).

6.1 Periodic Variations

The interpretation of data on η Car is complicated by the fact that different types of observation often refer to physically separate regions of the object. Optical aperture photometry refers mainly to the integrated light from the homunculus. This light is believed to be dust-scattered radiation from the central object. The mid-infrared ($\sim 10\mu\text{m}$) radiation is mainly dust emission from the homunculus. Near infrared ($\sim 2\mu\text{m}$) radiation comes from a region much more concentrated to the central object than the optical light. The rich, sharp, emission line spectrum which is so prominent on ground-based slit spectra of the central region and shows the high/low excitation states discussed above, has been found from HST observations (Davidson et al. 1997) to come, not from the central object itself, but from nebular knots (their B, C, D) about 0.2 arcsec away.

The new epochs of low excitation reported in section 2 together with those already known are clearly consistent with the periodicity of 2020 days suggested by Daminieli et al., at least over the last 50 years. As already noted, Daminieli et al. (1997) found radial velocity changes in the $\text{Pa}\gamma$ line which they suggested were due to motion of a star (the primary) in a highly eccentric binary orbit. In this orbit periastron is within 0.001 of inferior conjunction. Davidson et al. (2000) point out that much of the emission observed in $\text{Pa}\gamma$ from the ground comes from surrounding nebulosity, not the

central object itself. Their HST observations at two epochs do not support the Daminieli et al. orbit.

Despite the results of Davidson et al. (2000), a binary model of some kind is still probably the most satisfactory explanation of the 2020 day periodicity. Such a conclusion is supported by the infrared and X-ray dips which seem to point to some sort of eclipse phenomenon. Whitelock & Laney (1999) noted that the infrared light curve bore a rather striking qualitative resemblance to the optical light curve of some classical cataclysmic variables where a dip is superposed on a ‘hump’ in the light curve (see section 5 and Fig. 6 of the present paper). In these systems much of the light is due to a hot spot on a disc around a white dwarf; the spot being heated by infalling matter from a secondary star. The hump is due to the varying aspect of the spot as it moves in the orbit and the dip is due to its eclipse by the secondary. The infrared (Fig. 7) and X-ray (Ishibashi et al. 1999) light curves of η Car even show evidence of a two step structure similar to that seen in the eclipse light curves of some cataclysmic variables (e.g. Z Cha, see Cook & Warner 1984). In the case of η Car the ‘hot spot’ could either be on a disc or else be a hot region in an interacting wind model and the eclipse due either to an optically thick plasma or a star. This type of model does not necessarily require an eccentric orbit. It remains to be determined how much the ‘hot spot’ contributes to the total luminosity of the system. The depth of the eclipse shows that at least 20 percent of the near-infrared flux and essentially all of the X-ray flux is generated in the ‘hot spot’.

Davidson (1997) has suggested that the modulation of the near infrared flux in the 2020 day cycle is due to variation in free-free emission. This is evidently consistent with a ‘hot spot’ model. Smith & Gehrz (2000) find, from high resolution images, that the flux near $2\mu\text{m}$ was more centrally concentrated when the object was brighter at this wavelength, though it is not entirely clear how much this is related to the 2020 day periodicity and how much to the secular variations. The sharp emission-line spectrum, coming from a region separated from the central object, is presumably at least partially excited by radiation from the ‘hot spot’. This spectrum will thus vary, in the 2020 day cycle, according to the relative positions of the spot (and/or its intensity) and the excited region. Hence the orbit must be eccentric, unless the ejecta responsible for the sharp line spectra are distributed asymmetrically about the central object. Davidson et al. (1997) show that the ejecta (C,D) are moving towards us relative to the central object indicates that this latter condition is fulfilled.

It would appear to be significant that the phase and duration of the eclipse is the same as that of the low excitation state. Any phase offset between the two is quite small. The X-ray flux which is being eclipsed is presumably generated in the ‘hot spot’, the sharp emission lines come from a region separated from this. The infrared flux may come from either or both these regions. The similar lengths of the eclipse and of the low excitation state imply that the emission-line region can only subtend a small angle as seen from the central source. Furthermore, the fact that these two phenomena occur at the same phase indicates that the direction from the central source to the emission-line region(s) can only make a small angle with the line of sight from the central source to the observer. Davidson et al. (1997) show that the emis-

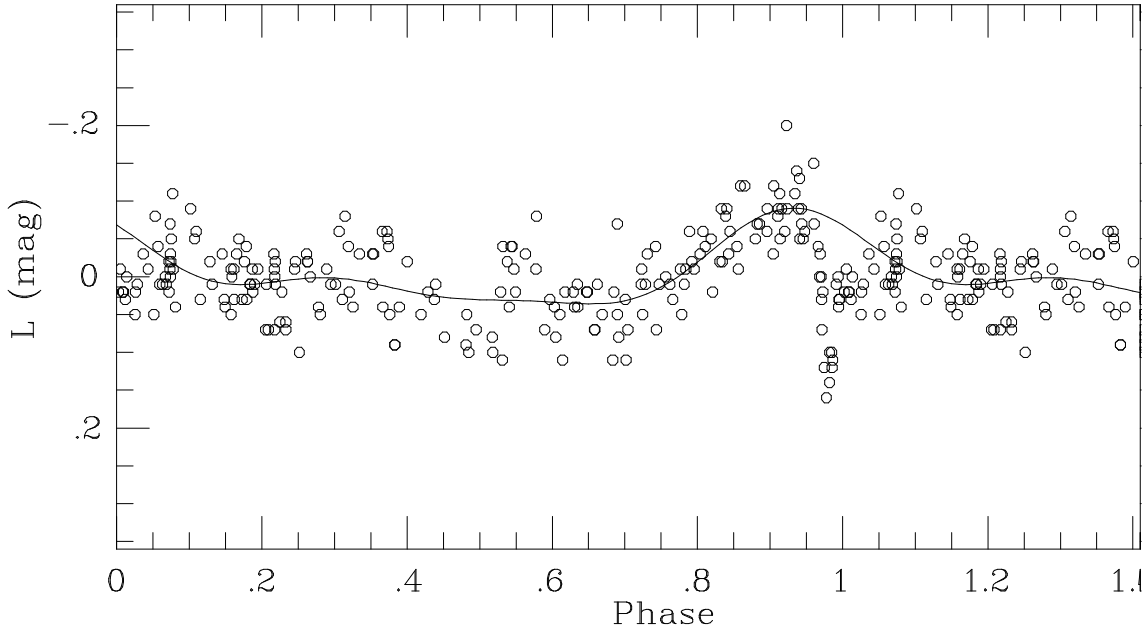


Figure 6. The phased light curve at L , assuming a period of 2020 day and with a linear trend, of $0.002 \text{ mag yr}^{-1}$, removed. A third order sine fit is shown ($\sigma = 0.042 \text{ mag}$).

sion line regions C and D lie in the equatorial plane of the bipolar system. This is evidently consistent with our eclipse model since we would expect the orbital plane of the binary to coincide with the plane of symmetry of the bipolar lobes. The inclination of the equatorial plane to the plane of the sky is $i = 57^\circ \pm 10^\circ$ (Davidson & Humphreys 1997). Stevens & Pittard (1999) obtained significant X-ray eclipses in a model which adopted $i = 60^\circ$ consistent with this. However the referee (Professor Davidson) informs us that Davidson et al. (to be published) have used HST/STIS data to revise the inclination from 57° to 40° which makes it more difficult to maintain an eclipse model with the orbit in this plane.

We have stressed the hot-spot model because the observed light curve is strikingly similar to that of a cataclysmic variable, though on a vastly different scale. Evidently this model must remain speculative pending a quantitative approach. The referee has in fact suggested that one should consider an alternative model (Davidson 1999) in which the spectroscopic low states etc. are the result of a secondary star entering a circumstellar disc round the primary or else inducing sudden mass ejection from the primary.

6.2 Secular Variations

The gradual brightening of the η Car system over much of the 20th century has generally been attributed to a gradual decrease in reddening as the dust formed in the great eruption dissipates. Whilst this seems plausible as a general explanation, the details are undoubtedly complex. Over the last 30 years, at least, the object has brightened by about the same amount in JHK as in the visual region and this has suggested a large-particle model (neutral extinction). However, the visual brightness, as normally estimated, is dominated by scattered light from the homunculus whereas the JHK emission is more concentrated to the central object. It is not entirely clear how the visual brightness of the

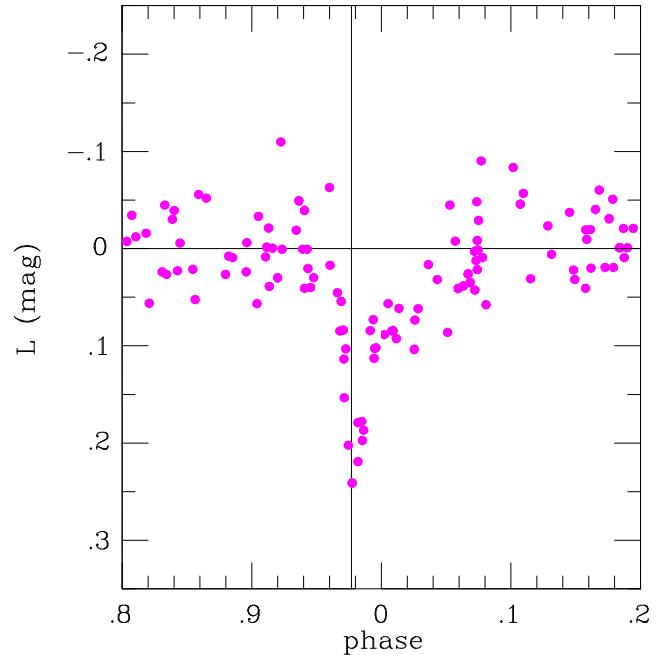


Figure 7. The L light curve from phase 0.8 to 0.2 with a linear trend and the third order sine curve of Fig. 6 removed.

homunculus will change as it expands and both absorption and scattering decrease. The recent increase in the rate of brightening (Davidson et al. 1999) is in any case incompatible with a simple model of decreasing absorption due to the steady expansion of a dust shell. Furthermore it is striking that this increase is similar in the visual and near infrared. It remains possible that some of the observed variations are due to changes in the central engine itself, as suggested in Paper I, and this would seem possible on a ‘hot spot’ model.

That the brightening is not simply due to the clearing

of obscuration is also evident from the fact that there are long term physical changes in the system. Not only is the homunculus expanding, but the ejecta which contribute the sharp-line spectrum are moving away from the central object (Davidson et al. 1997) and are undergoing long term changes which were reviewed in section 2. The secular increase in the strength of He I reflects an increase in excitation. The evidence also suggests an increase in $[\text{Fe II}]/\text{Fe II}$ between 1899 and 1913 which presumably indicates a decrease in density in the emitting region. This ratio does not seem to have changed significantly since 1913.

7 CONCLUSIONS

The photometric and spectroscopic results discussed in this paper seem most naturally explicable by an interacting-binary model of some kind. A binary model involving a ‘hot spot’ is basically that proposed originally by Bath (1979); though the long period presumably indicates that in the case of η Car, the interaction involves a stellar wind from at least one of the stars rather than Roche-lobe overflow. It is evident that a full quantitative model of the η Car system is still a matter for the future. However the results of the present paper provide considerable constraints for any such model.

Acknowledgements

We are grateful to Dave Laney, Tom Lloyd Evans, Enrico Olivier and Ronald Heijmans for making some of the *JHKL* observations. The re-examination of the archival spectra arose out of discussions with Roberta Humphreys. We thank the referee (Kris Davidson) for some pertinent comments. This paper is based partly on observations made from the South African Astronomical Observatory.

REFERENCES

- Aitken D.K., Jones B., Bregman J.D., Lester D.F., Rank D.M., 1977, *ApJ*, 217, 103
 Aller L.H., Dunham T., 1966, *ApJ*, 146, 126
 Altamore A., Maillard J.-P., Viotti R., 1994, *A&A*, 292, 208
 Bath G.T., 1979, *Nature*, 282, 274
 Baxandall F.E., 1919, *MNRAS*, 79, 619
 Bidelman W.P., Galen T.A., Wallerstein G., 1993, *PASP*, 105, 785
 Carter B.S., 1990, *MNRAS*, 242, 1
 Cook M.C., Warner B., 1984, *MNRAS*, 207, 705
 Daminieli A., 1996, *ApJ*, 460, L49
 Daminieli A., Viotti R., Cassatella A., Baratta G.B., 1994, *SSR*, 66, 211
 Daminieli A., Conti P.S., Lopes D.F., 1997, *New Ast.*, 2, 107
 Daminieli A., Stahl O., Kaufer A., Wolf B., Quast G., Lopes D.F., 1998, *A&AS*, 133, 299
 Daminieli A., Viotti R., Kaufer A., Stahl O., Wolf B., de Araújo F.X., 1999, in: *Eta Carinae at the Millennium*, J.A. Morse et al. (eds.), *ASP Conf. Ser.*, 179, p. 196
 Daminieli A., Kaufer A., Wolf B., Stahl O., Lopes D.F., de Araújo F.X., 2000, *ApJ*, 528, L101
 Davidson K., 1997, *New Ast.*, 2, 387
 Davidson K., 1999, in: *Eta Carinae at the Millennium*, J.A. Morse et al. (eds.) *ASP Conf. Ser.*, 179, 304
 Davidson K., Humphreys R.M., 1997, *ARAA*, 35, 1
 Davidson K., et al., 1997, *AJ*, 113, 335
 Davidson K., et al., 1999, *AJ*, 118, 1777
 Davidson K., Ishibashi K., Gull T.R., Humphreys R.M., Smith N., 2000, *ApJ*, 530, L107
 Gaviola E., 1953, *ApJ*, 118, 234
 Gill D., 1901, *Proc. Roy. Soc. (Lond)* 68, 456 and 1901, *MNRAS*, 61, Appendix p. 66
 Hillier D.J., Allen D.A., 1992, *A&A*, 262, 153
 Ishibashi K., Corcoran M.F., Davidson K., Swank J.H., Petre R., Drake S.A., Daminieli A., White S., 1999, *ApJ*, 524, 983
 Lunt J., 1919, *MNRAS*, 79, 621
 McGregor P.J., Rathborne J.M., Humphreys R.M., in: *Eta Carinae at the Millennium*, J.A. Morse et al. (eds.) *ASP Conf. Ser.*, 179, p. 236
 Moore J.H., Sanford R.F., 1913, *Lick Obs. Bull.* 8, 55 (No. 252)
 Morse J.A., Humphreys R.M., Daminieli A., (eds.), 1999, *Eta Carinae at the Millennium*, *ASP Conf. Ser.*, 179
 Rodgers A.W., Searle L., 1967, *MNRAS*, 135, 99
 Smith N., Gehrz R.D., 2000, *ApJ*, 529, L99
 Spencer Jones H., 1931, *MNRAS*, 91, 794
 Stevens I.R., Pittard J.M., 1999, in: *Eta Carinae at the Millennium*, J.A. Morse et al. (eds.) *ASP Conf. Ser.*, 179, p. 295
 Thackeray A.D., 1953, *MNRAS*, 113, 211
 Thackeray A.D., 1967, *MNRAS*, 135, 51
 Thackeray A.D., 1977, *Mem.RAS*, 83,1
 van Genderen A.M., Sterken C., de Groot M., Burki G., 1999, *A&A*, 343, 847
 Viotti R., 1968, *Mem. Soc. Ast. It.*, 39, 105
 Walborn N.R., Liller M.H., 1977, *ApJ*, 211, 181
 Westphal J.A., Neugebauer G., 1969, *ApJ*, 156, L45
 Whitelock P.A., Feast M.W., Carter B.S., Roberts G., Glass I.S., 1983, *MNRAS*, 203, 385, Paper I
 Whitelock P.A., Feast M.W., Koen C., Roberts G., Carter B.S., 1994, *MNRAS*, 270, 364, Paper II
 Whitelock P.A., Laney C.D., 1999, in: *Eta Carinae at the Millennium*, J.A. Morse et al. (eds.) *ASP Conf. Ser.*, 179, p. 258
 Wolf B., Kaufer A., Stahl O., Daminieli A., 1999, in: *Eta Carinae at the Millennium*, J.A. Morse et al. (eds.), *ASP Conf. Ser.*, 179, p. 243
 Zanella R., Wolf B., Stahl O., 1984, *A&A*, 137, 79